

Photochemistry of cyclohexene oxide radical cations in freonic matrices at 77 K

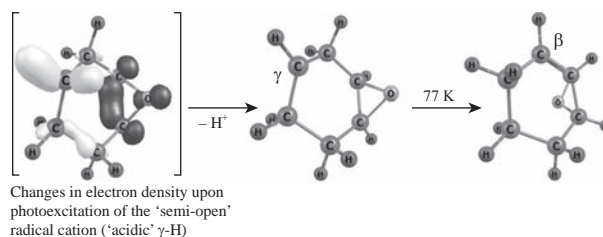
Ivan D. Sorokin,* Oleg I. Gromov, Vladimir I. Pergushov, Daria A. Pomogailo and Mikhail Ya. Mel'nikov

Department of Chemistry, M. V. Lomonosov Moscow State University, 119991 Moscow, Russian Federation.

E-mail: ivan.d.sorokin@gmail.com

DOI: 10.1016/j.mencom.2018.11.018

By employing EPR and UV/VIS spectroscopy and quantum chemical techniques, we demonstrated that the radical cations of cyclohexene oxide were stabilized upon radiolysis in freonic matrices at 77 K in their distorted form (with the C–C bond in the oxirane fragment elongated to 0.179 nm). Upon the action of light in the absorption band of these radical cations ($\lambda_{\max} \sim 480\text{--}490\text{ nm}$), they undergo deprotonation, successively yielding 7-oxabicyclo[4.1.0]heptan-3-yl and 7-oxabicyclo[4.1.0]heptan-2-yl radicals.



When deciphering the photochemical pathways of transformation for radical ionic radiolysis products in their matrix-stabilized state, the interpretation of experimental spectroscopic data is complicated by many aspects, which hinders elucidating universal patterns in such reactions for matrices of varying properties, even for smaller species. These data are crucial in predicting the behavior of materials under extreme conditions (when treated with ionizing radiation or light and/or at low temperatures). Thus, for several radical cations (RCs) of methyloxiranes stabilized in freons at 77 K,^{1–5} reversible phototransformations were found, manifesting in an exchange between the cyclic and ring-open forms of those RCs. Reversible photocyclization was also detected for related methylthiirane RCs under the same conditions,⁶ while the photochemical behavior of the aziridine RC was different: the action of light provoked irreversible ring opening in the cyclic structure.⁷ Additionally, it was demonstrated^{3,5} that the presence of geminal methyl groups in the structures of RCs derived from methyloxiranes disallowed photocyclization. The aim of this work was to study the phototransformations of RCs with an oxirane fragment in their structure along new mechanistic pathways.

Earlier,⁸ it was noted that cyclohexene oxide/ CFCl_3 solutions were violet upon irradiation at 77 K, indirectly pointing to the formation of ring-open pseudoallylic RCs. However, the detected EPR spectrum did not make it possible to determine the nature of paramagnetic species stabilized under those conditions. In this study, a CFCl_3 matrix was employed along with CF_3CCl_3 and $\text{CF}_2\text{CICFCl}_2$.[†]

Calculations have been performed by means of the unrestricted DFT method using the ORCA 3.0.3 program package.¹⁰ B3LYP functional together with the full-electron def2-TZVP basis set¹¹ have been used to calculate the geometry of potential energy

[†] Experimentally, CFCl_3 (~99%, Aldrich), $\text{CF}_2\text{CICFCl}_2$ (~99%, Aldrich) and CF_3CCl_3 (>99% according to NMR data, obtained from ~99% Aldrich $\text{CF}_2\text{CICFCl}_2$ using a known procedure⁹) have been employed as matrices. Cyclohexene oxide (~98%, Aldrich) was used without additional purification. The sample preparation procedures, irradiation techniques, detection methodology related to EPR and optical absorption spectra and the procedure of the photochemical experiment have been described earlier.³

surface minima. Geometries at minima and transition states have been additionally checked for the presence of imaginary vibration frequencies. The spin-Hamiltonian parameters have been calculated using the B3LYP functional together with the full-electron N07D basis set.¹²

The calculations carried out for the cyclohexene oxide RC demonstrate that, upon ionization, the following forms can be yielded (Figure 1): cyclic form **1**, distorted cyclic form **2** with an elongated C–C bond in the oxirane ring and ring-open form **3** with C–C cleavage in the oxirane ring. Note that ring-open form **3** was the most stable among the listed structures (Table 1). The computations showed that the height of a barrier on the **1** \rightarrow **2** transformation pathway did not exceed 5 kJ mol⁻¹; therefore, the stabilization of **1** under irradiation conditions at 77 K seemed unlikely. Furthermore, according to the calculation results, the

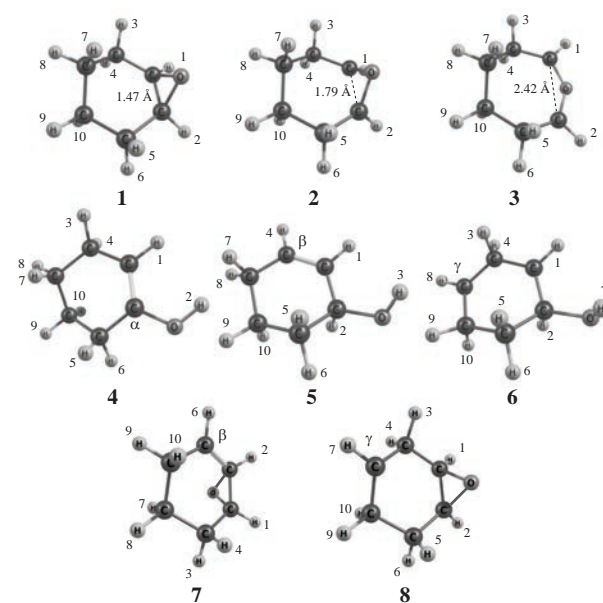


Figure 1 Calculated (DFT/B3LYP/NO7D) structures of cyclohexene oxide-derived RCs (**1–3**), distonic RCs formed upon H^+ transfer (**4–6**) and radicals yielded upon H^+ extraction (**7, 8**).

Table 1 DFT/B3LYP/NO7D calculation results for full energies, isotropic hfc constants with hydrogen nuclei (mT) and *g*-tensor components of the CHO-derived RCs and radicals.^a

RC	Magnetic resonance parameters										<i>E</i> /kJ mol ⁻¹
	<i>a</i> _{iso} (H ¹)	<i>a</i> _{iso} (H ²)	<i>a</i> _{iso} (H ³)	<i>a</i> _{iso} (H ⁴)	<i>a</i> _{iso} (H ⁵)	<i>a</i> _{iso} (H ⁶)	<i>a</i> _{iso} (H ⁷)	<i>a</i> _{iso} (H ⁸)	<i>a</i> _{iso} (H ⁹)	<i>a</i> _{iso} (H ¹⁰)	
1	0.21	5.48	0.52	0.20	0.31	0.62	0.64	<0.1	3.04	<0.1	226.4
2	0.47	<0.1	4.62	1.34	2.77	<0.1	<0.1	<0.1	<0.1	<0.1	195.1
3	1.67	1.66	0.84	3.42	3.42	0.83	<0.1	<0.1	<0.1	<0.1	110.4
4	1.49	0.45	2.87	5.75	1.86	0.56	0.13	<0.1	<0.1	<0.1	0.0
5	0.18	4.45	0.36	0.32	0.26	0.31	2.88	1.93	1.47	<0.1	109.7
6	1.60	2.09	2.38	0.55	0.24	<0.1	<0.1	1.47	1.03	2.77	194.8
7	0.41	0.13	0.12	<0.1	–	2.21	<0.1	<0.1	2.28	4.35	–
8	<0.1	<0.1	0.81	4.42	0.10	<0.1	2.40	–	0.22	4.28	–

^aFull energies are not given for structures of different stoichiometry (7, 8).

products of intramolecular hydrogen atom transfer in the cyclohexene oxide RC, associated with the C–O bond in the oxirane cycle undergoing cleavage, was more stable than the cyclic forms of RC (1–3) in the case of structures 4 and 5, while product 6 lied significantly higher on the energy scale.

Upon X-ray irradiation of the frozen cyclohexene oxide/CF₃CCl₃ solutions (0.3–0.5 mol%) at 77 K, a seven-line signal with splittings of 1.3–1.8 mT was observed in the EPR spectrum [Figure 2(a)]. The resolution improved significantly upon warming the sample to 110 K [Figure 2(b)]. Upon radiolysis, induced absorption arose in the UV/VIS spectrum in the region of $\lambda \approx 380$ –750 nm with a maximum at 480–490 nm. An analogous seven-line EPR spectrum was also detected upon the X-ray irradiation of cyclohexene oxide/CF₂CICFCl₂ solutions at 77 K. On the other hand, in the CFCl₃ matrix, an eleven-line spectrum was detected upon X-ray irradiation under the same conditions. Interestingly, the location of the induced absorption maximum

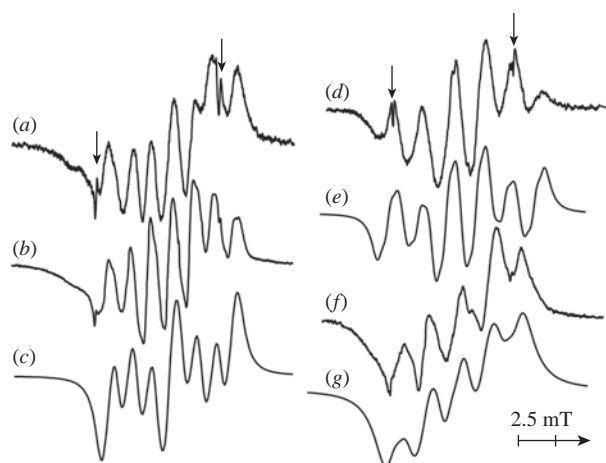


Figure 2 EPR spectra detected in irradiated cyclohexene oxide/CF₃CCl₃ solutions (a) immediately upon X-ray irradiation at 77 K and subsequent warming to 110 K: (b) experimental, (c) simulation with DFT-calculated parameters of form 2, and upon the action of light with $\lambda = 546$ nm at 77 K: (d) difference spectrum of species yielded upon photolysis and subsequently perishing at 77 K, (e) simulation, optimized parameters of 8; (f) experimental spectrum detected upon further storage of the sample at 77 K, and (g) simulation, optimized parameters of 7. Arrows point to the third and the fourth components of the hyperfine structure of the additional Mn²⁺ ions in MgO powder. Magnetic resonance parameters for spectra are discussed in the text.

(480–490 nm) in the UV/VIS spectrum for this matrix was close to that observed in the CF₃CCl₃ matrix.

Thus, upon the radiolysis of cyclohexene oxide/Freon solutions, induced absorption in the experimental UV/VIS spectra arose in the region of $\lambda \approx 380$ –750 nm with maxima at 480–490 nm. Upon the photobleaching of matrix-derived intermediates (ion pairs)¹³ and the subsequent action of light with $\lambda = 546$ nm, the absorption band at 480–490 nm perished irreversibly in CFCl₃ and CF₃CCl₃. Note that, in CF₃CCl₃, this band overlapped with another one lying in a shorter-wave region and associated with matrix-derived intermediates,¹³ while the resulting difference spectrum in the matrix of CFCl₃ (Figure 3) could be considered virtually individual. Correspondingly, the initial signals in the EPR spectra (the seven-line signal in CF₃CCl₃ and CF₂CICFCl₂ and the eleven-line signal in CFCl₃) perished completely upon photolysis, which allowed us to assign the absorption band with its maximum at 480–490 nm ($\epsilon_{490} \approx 5.6 \times 10^3$ dm³ cm⁻¹ mol⁻¹ in CF₃CCl₃, $\epsilon_{490} \approx 4.7 \times 10^3$ dm³ cm⁻¹ mol⁻¹ in CFCl₃) to the cyclohexene oxide RC. The magnetic resonance parameters calculated by means of DFT for the cyclohexene oxide RC with the elongated C–C bond (Table 1, RC 2) allowed us to successfully fit the seven-line signal in the EPR spectrum that was detected in CF₃CCl₃ upon radiolysis [Figure 2(c)]. For enhanced quality in our fitting of the eleven-line EPR signal, we had to slightly amend the hfc values calculated for 2 [*a*(1H): 5.16, 1.18, 0.91 and 3.15 mT] while maintaining the values of *g*-tensor components given in Table 1. This kind of attribution for the EPR spectra, together with the observed absorption spectra being virtually identical in different matrices, allows us to confidently

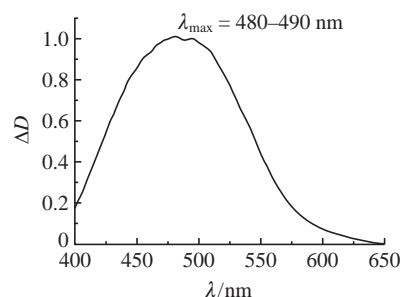


Figure 3 Difference UV/VIS spectrum detected in irradiated cyclohexene oxide/CFCl₃ solutions upon the action of light with $\lambda = 546$ nm at 77 K.

state that form **2** of the cyclohexene oxide RC is generated and stabilized upon X-ray irradiation of cyclohexene oxide solutions in freonic matrices. We entertained a hypothesis wherein two conformers of **2** with varying magnetic resonance parameters could be stabilized at the same time. This attribution and the corresponding fitting would have resulted in a practically perfect reproducibility for experimentally detected integral intensities in the EPR spectra for different matrices. Unfortunately, the DFT calculations do not provide us with the necessary structures that could be characterized by the required sets of hfc constants. However, this suggestion does not make our conclusion about **2** being stabilized in irradiated cyclohexene oxide/Freon solutions unjustified.

The paramagnetic products afforded by the cyclohexene oxide RC upon photolysis do not absorb visible light. Therefore, they are either distonic radical cations or neutral radicals. The EPR spectrum detected immediately upon the photolysis of the irradiated cyclohexene oxide/CF₃CCl₃ solutions can be interpreted as the sum of a six-line signal [Figure 2(d)] and a five-line signal [Figure 2(f)] with splittings of 2.2 and 1.9 mT, respectively. Importantly, the six-line signal quantitatively transforms into the five-line one at 77 K in a single day.

Calculated parameters of distonic RCs **4–6**, as well as those for cyclic RC form **1** (with the shorter C–C bond) and ring-open form **3** (Table 1), do not allow for assigning any of the EPR spectra, which enabled us to exclude the possibility of these species being formed as photolysis products. Due to that, neutral radicals were explored as possible transformation products, hypothetically yielded upon deprotonation in the cyclohexene oxide RC. DFT calculations were carried out for magnetic resonance parameters in those species. A change in electron density upon photoexcitation in **2**, found in our TD-DFT calculations and leading to increased acidity for the γ -H atom (as compared to other hydrogen atoms in **2**), substantiates the hypothesis of photolysis proceeding along a deprotonation pathway.

Thus, the six-line EPR spectrum detected upon photolysis of the cyclohexene oxide RC [Figure 2(d)] can be fitted [Figure 2(e)] with the parameters [$a_1(1H) = 4.44$ mT, $a_2(1H) = 4.31$ mT, $a_3(1H) = 2.25$ mT, $a_4(1H) = 0.69$ mT, and $a_5(1H) = 0.48$ mT] found by optimizing the hfc constants calculated for 7-oxabicyclo[4.1.0]heptan-3-yl radical **8** (Table 1). Correspondingly, the five-line EPR spectrum [Figure 2(f)] detected in the current system as pertaining to the ultimate product of transformations can be fitted [Figure 2(g)] by optimizing the hfc constants [$a_1(1H) = 4.17$ mT, $a_2(1H) = 2.29$ mT, $a_3(1H) = 1.75$ mT, and $a_4(1H) = 0.84$ mT] calculated for 7-oxabicyclo[4.1.0]heptan-2-yl radical **7**.

Based on the data explored, we can propose the following transformation mechanism for RC **2** with the elongated C–C bond in the oxirane cycle stabilized upon X-ray irradiation: under the action of light with $\lambda = 546$ nm, the deprotonation of **2** occurs, followed by 1,2-migration of a hydrogen atom, which results in **8** yielding **7**. The latter reaction can only proceed *via* tunnelling in our experimental setup¹⁴ since estimates suggest

that the height of the activation barrier for this type of hydrogen atom 1,2-migration exceeds 160 kJ mol⁻¹. The quantum yields of phototransformations for RC **2** estimated from the kinetics of their decay are relatively low and amount to $\phi_{546} = 0.02$ (in CF₃CCl₃) and 0.06 (in CFCl₃). According to a suggestion formulated for tetrahydrofuran RC,¹⁵ which was then supported experimentally,¹⁶ these calculated quantum yields indicate that proton transfer to the substrate molecules is quite likely.

We are grateful to Professor V. I. Feldman for fruitful discussions.

This work was supported by the Russian Foundation for Basic Research (project no. 16-03-00029) and carried out with the use of equipment purchased on behalf of the Development Program of Moscow State University. Calculations have been performed using the resources of the Supercomputing Center of M. V. Lomonosov Moscow State University.¹⁷

References

- 1 K. Ushida, T. Shida and K. Shimokoshi, *J. Phys. Chem.*, 1989, **93**, 5388.
- 2 M. Lindgren and M. Shiotani, in *Radical Ionic Systems. Properties in Condensed Phases. ESR Studies of Radical Cations of Cycloalkanes and Saturated Heterocycles*, eds. A. Lund and M. Shiotani, Kluwer Academic, Dordrecht, 1991, vol. 6, pp. 125–150.
- 3 I. D. Sorokin, V. I. Feldman, O. L. Mel'nikova, V. I. Pergushov, D. A. Tyurin and M. Ya. Mel'nikov, *Mendeleev Commun.*, 2011, **21**, 153.
- 4 I. D. Sorokin, V. I. Feldman, O. L. Mel'nikova, V. I. Pergushov, D. A. Tyurin and M. Ya. Mel'nikov, *Mendeleev Commun.*, 2011, **21**, 155.
- 5 I. D. Sorokin, O. L. Melnikova, V. I. Pergushov, D. A. Tyurin, V. I. Feldman and M. Ya. Melnikov, *High Energy Chem.*, 2012, **46**, 183 (*Khim. Vys. Energ.*, 2012, **46**, 228).
- 6 I. D. Sorokin, O. I. Gromov, I. S. Zharinova, V. I. Pergushov and M. Ya. Mel'nikov, *Mendeleev Commun.*, 2017, **27**, 479.
- 7 I. D. Sorokin, O. I. Gromov, V. I. Pergushov and M. Ya. Mel'nikov, *Mendeleev Commun.*, 2016, **26**, 332.
- 8 J. Rideout, M. C. R. Symons and B. W. Wren, *J. Chem. Soc., Faraday Trans. 1*, 1986, **82**, 167.
- 9 W. T. Miller, E. W. Fager and P. H. Griswald, *J. Am. Chem. Soc.*, 1950, **72**, 705.
- 10 F. Neese, *Wiley Interdiscip. Rev.: Comput. Mol. Sci.*, 2012, **2**, 73.
- 11 F. Weigend and R. Ahlrichs, *Phys. Chem. Chem. Phys.*, 2005, **7**, 3297.
- 12 V. Barone, P. Cimino and E. Stendardo, *J. Chem. Theory Comput.*, 2008, **4**, 751.
- 13 M. Ya. Melnikov, D. V. Baskakov and V. I. Feldman, *High Energy Chem.*, 2002, **36**, 309 (*Khim. Vys. Energ.*, 2002, **36**, 346).
- 14 V. I. Feldman, S. M. Borzov, F. F. Sukhov and N. A. Slovokhotova, *Khim. Fiz.*, 1988, **7**, 781 (in Russian).
- 15 V. I. Fel'dman and M. Ya. Mel'nikov, *High Energy Chem.*, 2000, **34**, 236 (*Khim. Vys. Energ.*, 2000, **34**, 279).
- 16 K. S. Taletskiy, V. I. Borovkov, L. N. Shchegoleva, I. V. Beregovaya, V. A. Bagryansky and Yu. N. Molin, *Dokl. Phys. Chem.*, 2014, **455**, 41 (*Dokl. Akad. Nauk*, 2014, **455**, 171).
- 17 V. Sadovnichy, A. Tikhonravov, V. Opanasenko and V. Voevodin, in *Contemporary High-Performance Computing: from Petascale toward Exascale*, ed. J. S. Vetter, CRC Press, Boca Raton, 2013, p. 283.

Received: 14th May 2018; Com. 18/5577